Journal of Chromatography B, 875 (2008) 200–207

Contents lists available at ScienceDirect

Journal of Chromatography B

journal homepage: www.elsevier.com/locate/chromb

Exploring enantiospecific ligand–protein interactions using cellular membrane affinity chromatography: Chiral recognition as a dynamic process☆

Krzysztof Jozwiak[a], Ruin Moaddel[b], Sarangan Ravichandran[c], Anita Plazinska[a], Joanna Kozak[a], Sharvil Patel[b,d], Rika Yamaguchi[b,e], Irving W. Wainer[b,*]

[a] Laboratory of Drug-Receptor Interactions, Medical University of Lublin, 20-081 Lublin, Poland
[b] Gerontology Research Center, National Institute on Aging, National Institutes of Health, 5600 Nathan Shock Drive, Baltimore, MD 21224-6825, USA
[c] Advanced Biomedical Computing Center, National Cancer Institute-Frederick/SAIC, Frederick, MD 21702, USA
[d] Cadilia Healthcare Ltd., Ahmedabad 380015, Gujarat, India
[e] Shionogi & Co., Ltd., Hyogo 660-0813, Japan

ARTICLE INFO

Article history:
Received 6 May 2008
Accepted 14 July 2008
Available online 9 August 2008

Keywords:
Nicotinic acetylcholine receptors
Organic cation transporters
Pharmacophore modeling
Non-linear chromatography
Molecular modeling

ABSTRACT

The chiral recognition mechanisms responsible for the enantioselective binding on the $\alpha_3\beta_4$ nicotinic acetylcholine receptor ($\alpha_3\beta_4$ nAChR) and human organic cation transporter 1 (hOCT1) have been reviewed. The results indicate that chiral recognition on the $\alpha_3\beta_4$ nAChR is a process involving initial tethering of dextromethorphan and levomethorphan at hydrophobic pockets within the central lumen followed by hydrogen bonding interactions favoring dextromethorphan. The second step is the defining enantioselective step. Studies with the hOCT1 indentified four binding sites within the transporter that participated in chiral recognition. Each of the enantiomers of the compounds used in the study interacted with three of these sites, while (*R*)-verapamil interacted with all four. Chiral recognition arose from the conformational adjustments required to produce optimum interactions. With respect to the prevailing interaction-based models, the data suggest that chiral recognition is a dynamic process and that the static point-based models should be amended to reflect this.

1. Introduction

In 1858 Louis Pasteur demonstrated that *dextro*- and *levo*-ammonium tartate were metabolized at different rates by *Penicillium glaucum* mould [1]. These observations led Pasteur to the realization that stereochemistry in general and enantioselectivity in particular play key roles in the basic mechanisms of life [2]. One of the effects of stereochemistry is the different pharmacological response produced by the enantiomers of a chiral drug. This was initially demonstrated in 1908 by Abderhalde and Muller, who described the differential abilities of (+)- and (−)-epinephrine to raise blood pressure [1]. Since the publication of these observations, chirality and the molecular recognition of stereochemical differences have been active areas of research, cf. [3]. Currently, the determination of enantioselective interactions between a chiral drug and a biological system is an integral component of modern pharmacology and drug discovery [4].

The increased emphasis on drug stereochemistry has been stimulated, in part, by developments in the chromatographic and electrophoretic separation of enantiomers. Over the past 30 years, research into the analytical and preparative separation of drug stereoisomers has developed and brought to the market an impressive number of new technologies. These advances have transformed enantiomeric separations into a relatively simple and routine procedure. Professor Wolfgang Lindner was one of the pioneers in this field. He published his first papers on chiral ligand exchange chromatography in 1979 [5,6] and co-authored one of the initial reviews of the chromatographic separation of enantiomers in 1985 [7]. This manuscript is dedicated to him on the occasion of his 65th birthday as recognition of his contributions to the field of enantioselective separations.

2. Exploring chiral recognition using liquid chromatography

2.1. Chiral stationary phases

One of the strategies to identify and quantify enantioselective interactions is chiral liquid chromatography. In this approach, a chiral selector is placed in the mobile phase or incorporated into a

☆ This paper is part of the Special Issue 'Enantioseparations', dedicated to W. Lindner, edited by B. Chankvetadze and E. Francotte.

* Corresponding author. Tel.: +1 410 558 8498; fax: +1 410 558 8409.
E-mail addresses: Wainerir@grc.nia.nih.gov, wainerir@mail.nih.gov (I.W. Wainer).

1570-0232/$ – see front matter © 2008 Elsevier B.V. All rights reserved.
doi:10.1016/j.jchromb.2008.07.048

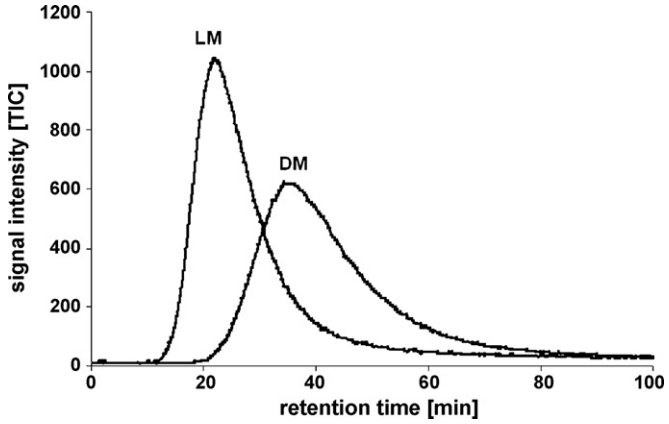

Fig. 1. The non-linear chromatography peak profiles obtained after the independent injection of dextromethorphan (DM) and levomethorphan (LM) on the CMAC ($\alpha_3\beta_4$ nAChR) column. In these experiments, the mobile phase was composed of ammonium acetate (10 mM, pH 7.4) modified with methanol in the ratio 85:15 (v/v), the flow rate was 0.2 ml/min and the experiments were carried out ambient temperature.

stationary phase to create a chiral stationary phase (CSP). A variety of small molecules and macromolecules have been used to create CSPs and the resulting columns have been used for analytical and preparative separations as well as for the study of the chiral recognition mechanisms. The biomolecules used to create CSPs have included small soluble carrier proteins such as acid α_1 glycoprotein [8] and serum albumins [9,10] and larger soluble proteins such as the enzymes α-chymotrypsin [11] and cellobiohydrolase I [12]. These CSPs have been recently reviewed [13,14]. Membrane-bound proteins, which include receptors, ion channel and drug transporters, have not been incorporated into CSPs. This is primarily due to the necessity of using membrane fragments containing the target protein in the creation of the CSP. The resulting stationary phases have poor chromatographic efficiencies, cf. Fig. 1 [15], and cannot be used in analytical separations.

2.2. Cellular membrane affinity chromatography

Recently, membrane-bound proteins, such as receptors, ion channels and drug transporters (Target Proteins), have been incorporated into chromatographic systems. In this approach, cellular membrane fragments obtained from cell lines expressing a Target Protein were used to create cellular membrane affinity chromatography (CMAC) columns. The resulting CMAC columns were used to study ligand binding to the Target Proteins as well as the functional consequences of the binding interactions. The general CMAC approach has been recently reviewed [16,17].

CMAC columns have been used with both zonal and frontal chromatographic techniques and in competitive displacement and temperature-dependent experiments. The data from these studies have demonstrated that the CMAC approach can be used to determine binding affinities (K_d values), the kinetics (k_{on} and k_{off}), the thermodynamics of the binding process and functional parameters such as IC_{50} and EC_{50} values and that the CMAC-derived values are comparable to those obtained using standard biochemical and pharmacological techniques [16,17].

These studies also demonstrated that the immobilized Target Proteins retained their inherent enantioselectivity and that the CMAC approach could be useful in the prediction and/or interpretation of the pharmacological behavior of tested chiral substances [15,18,19]. In addition, the chromatographic data obtained on the CMAC columns were coupled with molecular modeling and used to develop chiral recognition mechanisms describing the enantiospecific ligand–Target Protein interactions. This review will discuss this approach using the enantioselective interactions observed on CMAC columns derived from cell lines expressing nicotinic acetylcholine receptors (nAChRs) [15,18] and the human organic cation transporter 1 (hOCT1) [19,20], and the implications of the derived chiral recognition mechanisms to the understanding of enantioselecitve interactions.

3. Chiral recognition as enthalpy and entropy driven processes

3.1. Chrial recognition as a "three-point" interaction

The initial theoretical description of enantioselective interactions in biological systems was published by Easson and Stedman [21]. In their model, enantioselective differences arose from the differential binding of enantiomers to a defined three-dimensional site on a protein containing three non-equivalent binding sites. Chiral discrimination occurs when one of the enantiomers interacts with all three of the sites while the other does not, a "three-point" interaction (TPI) model. This model was used by Dalgliesh to describe the chiral resolution of amino acid enantiomers by cellulose paper chromatography [22] and by Pirkle as the basis of the chiral recognition mechanism operating on the CSPs developed in his laboratory [23]. The TPI mechanism has become the standard explanation for chromatographic enantioselectivity.

An elegant description of the TPI mechanism was published by Davankov [24] and included the following observations:

> "In order to recognize and, possibly, discriminate between two enantiomeric species, the chiral selector has to 'feel' the special configuration of the partners, i.e., identify its orientation along three axes of the space. Therefore, just as a matter of principle, a 'mathematical' formulation of conditions required (but not necessarily sufficient) for the chiral selector to recognize the enantiomers is that, at least three configuration-dependent active points of the selector molecule should interact with three complementary and configuration-dependent active points of the enantiomer molecule."

3.2. Conformational mobility in the chiral recognition process

While the TPI model has been widely used to explain enantioselective interactions, it has not been universally applied. A number of other explanations have been proposed including two contact-points [25,26], extended three-points [27] and four location [28] models. One of the problems associated with the general application of the TPI mechanism is the conformational mobility of the selector and selectants. This issue was highlighted by Del Rio and coworkers during a retrospective study of the enantioselective separations of 1-(4-halogeno-phenyl)-1-ethylamine derivatives on the Whelk-01 CSP [29]. Based upon the data, the authors concluded that the TPI mechanism "does not seem to be a general applicable rule, and only ligands with a few degrees of freedom and which do not accept multiple binding modes with the CSPs seem to respect this simplified model." The CSP and selectants in Del Rio's study were relatively small, and the problems with the direct utilization of the TPI mechanism are significantly greater with protein-based CSPs and conformationally mobile selectants.

This issue was recently addressed by Sundaresan and Abrol who developed a general model for protein-substrate stereoselectivity, the multi-site "stereocenter-recognition" (SR) model [30,31]. The SR model is essentially a topological approach that expands the concept of sites (a single moiety on the molecule) to locations (composed of more than one moiety on the molecule). In the

SR approach, a single location on the selectant may interact with multiple sites on the selector or multiple selectant locations may interact with a single selector site [30].

While the SR model is an important contribution to the understanding of the chiral recognition process, particularly in biological systems, it is essentially a reflection of the end product of the interactions and not the process that was necessary to reach this end. The authors recognized this and concluded that like the TPI model, the SR model "presents a static view of chiral recognition, without taking into account the dynamics of the process." [31]. While the SR model allows for conformational flexibility in the substrate molecule [31], it is not routinely included in chiral recognition mechanisms. This is due to both the computational difficulty in accomplishing this task and the historical development of the TPI model.

3.3. The contribution of enthalpy and entropy to the chiral recognition process

When the enantiomers of a chiral compound, *R*-selectant and *S*-selectant, are injected onto the column containing a CSP, there is the possibility that energetically different *R*-selectant–selector and *S*-selectant–selector complexes will be formed resulting in the separate elution of the *R*- and *S*-selectant. The observed enantioselectivity ratio (α) reflects differences in the Gibbs free energies ($\Delta\Delta G^\circ$) of the complexes formed between the two enantiomers and the chiral selector, cf. [24] and can be defined as

$$\Delta\Delta G^\circ = \Delta G^\circ_R - \Delta G^\circ_S = -RT \ \ln \frac{K_S}{K_R} = -RT \ \ln \ \alpha \quad (1)$$

where the two enantiomers are designated as *R* and *S*, *R* is the gas constant (1.9872 cal mol^{-1} K^{-1}), *T* is the temperature of experimental conditions in Kelvin, K_S and K_R are equilibrium constants for respective enantiomer–selector complexes, and α is the ratio of equilibrium constants as well as the chromatographically observed enantioselective separation.

The ΔG° of each enatiomer–selector complex is

$$\Delta G^\circ = \Delta H^\circ - T\,\Delta S^\circ \quad (2)$$

where ΔH° is the change in enthalpy and ΔS° is the change in entropy associated with the formation of the selectant–selector complex. Thus, the $\Delta\Delta G^\circ$ value can be experimentally determined using chromatographic results, Eq. (1), or temperature-based Van 't Hoff studies, Eq. (2).

Most chiral recognition mechanisms concentrate on enthalpy and measure the relative stabilities of the selectant–selector complexes while ignoring the entropic contributions to the formation of the complexes. This was recognized by Davankov [24] who observed that while the $\Delta\Delta G^\circ$ values associated with enantioselectivity include both contributions from both $\Delta\Delta H^\circ$ and $\Delta\Delta S^\circ$, the $\Delta\Delta H^\circ$ contribution usually dominates due to the positive or negative interactions associated with the TPI. However, Davankov also indicated that in some instances, the ΔS° associated with the formation of the selectant–selector complex may be abnormally great, so the value of $T\Delta\Delta S^\circ$ is comparable to or exceeds $\Delta\Delta H^\circ$.

It is more likely that the distinction between enthalpy-driven and entropy-driven molecular chiral recognition is only a reflection of the relative contributions of these parameters to a single process, and that interaction-based models have obscured this fact. This is illustrated by the chiral recognition mechanisms associated with the enantioselective interactions of dextromethorphan (DM) and levomethorphan (LM) with the CMAC ($\alpha_3\beta_4$ nAChR) and (*R*)- and (*S*)-verapamil, and associated compounds, with the CMAC (hOCT1).

4. Enantioselective binding of DM and LM to the CMAC ($\alpha 3\beta 4$ nAChR)

4.1. CMAC (nAChR) columns

Nicotinic acetylcholine receptors (nAChRs) are a family of ligand-gated ion channels found in the central and peripheral nervous systems that regulate synaptic activity [32,33]. nAChRs are formed by bringing together five separate transmembrane proteins (subunits), each containing a large extra-cellular N-terminal domain, four membrane spanning alpha helices (M1, M2, M3, and M4) and a small C-terminal domain [34]. The subunits are oriented around a central pore, the transmembrane ion channel, formed by the M2 helical segments [33]. To date, 12 different neuronal subunits have been identified, nine labeled alpha ($\alpha 2$–$\alpha 10$) and three labeled beta ($\beta 2$–$\beta 4$). These subunits form channels of a wide variety of homomeric (α_x nAChR; where $x = 7$–10) and heteromeric ($\alpha_x\beta_y$ nAChR; where $x = 2$–6, $y = 2$–4) subtypes. The subtypes are found in different locations of the central and peripheral nervous system and have different physiological and pharmacological functions including cognition, neurodegeneration, pain, anxiety, depression, cardiovascular and gastrointestinal action [17].

CMAC columns have been developed from a series of transfected cell lines expressing different $\alpha_x\beta_y$ nAChRs. The CMAC columns have been shown to retain the binding activities of the native nAChRs and could be used to assess K_d, k_{on} and k_{off}, IC_{50} and EC_{50} values of nAChR agonists and competitive antagonists [17,35]. The CMAC columns were also able to characterize and describe the binding of another class of nAChR active compounds known as allosteric non-competitive inhibitors (NCIs) [18,36]. NCIs bind at sites that are located predominantly within the membrane portion of the nAChR. The best characterized NCI binding site is located inside of the inner surface of the ion channel, the central luminal domain, at which compounds bind and block ion flux through the channel. This site has been studied using the CMAC approach and the enantioselective NCI activities of dextromethorphan (DM) and levomethorphan (LM) [18].

4.2. Description of the enantioselective binding of DM and LM to the CMAC ($\alpha_x\beta_y$ nAChRs)

Non-linear chromatography (NLC) studies on the CMAC ($\alpha_3\beta_4$ nAChR) using the NCI mecamylamine as the marker ligand and DM and LM as the displacers were used to demonstrated that both methorphan enantiomers bound at the same, single central lumen binding site [15,18]. In these studies, DM was retained longer than LM, $k' = 40.5$ and 25.0, respectively, with an α of 1.62, Fig. 1 [15]. The enantioselective separation was studied using the Van 't Hoff approach in which the effect of temperature on retention and enantioselectivity were determined, Table 1 [15]. The data indicate that the difference in the chromatographic retentions of DM and LM on the CMAC ($\alpha_3\beta_4$ nAChR) column was enthalpy driven, $\Delta\Delta H = -0.33$ kcal mol^{-1}, $\Delta\Delta S \sim 0.5$ cal mol^{-1} T^{-1}, Table 1. The free energy changes, $\Delta\Delta G^\circ$, calculated using the Van 't Hoff and chromatographic approaches were in agreement, -0.29 kcal mol^{-1} and -0.28 kcal mol^{-1}, respectively.

By definition, an affinity-based column, such as a CMAC column, contains small amount of affinity binding sites which are limited by the concentration of the protein on the column. In this case it is assumed that the concentration of the solute injected on the column is significantly higher than the amount of binding sites on the stationary phase, and that experiments are run under mass overload conditions with non-linear Langmuir type isotherms [37,38]. As a result, the observed chromatographic peaks are asymmetric with concentration dependent tailing. These effects can be ana-

Table 1
The results of thermodynamic, kinetic and functional characterization of the dextromethorphan (DM) and levomethorphan (LM) with $\alpha_3\beta_4$ nAChR

	DM	LM
Thermodynamics (Van 't Hoff)		
ΔH° (kcal mol^{-1})	−6.92 (±0.19)	−6.59 (±0.18)
ΔS° (cal mol^{-1} T^{-1})	−15.7 (±0.7)	−15.2 (0.6)
ΔG° (kcal mol^{-1})	−2.33 (±0.4)	−2.04 (±0.4)
Kinetics (non-linear chromatography)		
k'	61.30 (±0.27)	35.81 (±0.15)
k_{on} (μM^{-1} s^{-1})	23.66 (±0.61)	18.61 (±0.38)
k_{off} (s^{-1})	1.01 (±0.01)	1.549 (±0.002)
K_a (μM^{-1})	23.40 (±0.36)	12.01 (±0.23)
Functional activity (nicotine stimulated $^{86}Rb^+$ efflux)		
IC50 (μM)	10.1 (±1.10)	10.9 (±1.08)
% Recovery (after 7 min)	38.25 (±15.46)	63.30 (±16.08)
% Recovery (after 4 h)	76.20 (±4.51)	93.12 (±8.76)

Thermodynamic parameters (ΔH°, ΔS° and ΔG°) were determined in van 't Hoff temperature dependence study in chromatographic experiments using equation: $\ln k' = (\Delta S^\circ/R) - ((\Delta H^\circ/R)(1/T))$; kinetic parameters were determined using the input impulse solution [40] for zonal non-linear chromatography using immobilized $\alpha_3\beta_4$ nAChR column (temperature of experiment 25 °C); functional parameters described actual blocking activity of ligand against $\alpha_3\beta_4$ nAChR using nicotine stimulated $^{86}Rb^+$ efflux assay.

lyzed using NLC techniques and the binding interactions between a ligand and the immobilized protein characterized through the calculation of the association rate constant (k_{on}), dissociation rate constant (k_{off}) for the ligand–receptor complex and the equilibrium constant for complex formation (K_a) [37,38].

The concentration-dependent peak profiles obtained during the NLC experiments on the CMAC ($\alpha_3\beta_4$ nAChR) column were analyzed using the impulse input solution for the mass balance equation [39] and the k_{on}, k_{off} and K_a were calculated for both enantiomers, Table 1. The data indicate that the k_{off} for the dissociation of the DM-$\alpha_3\beta_4$ nAChR complex was 53% lower than that calculated for the LM-$\alpha_3\beta_4$ nAChR complex, and suggest that slower dissociation kinetics is the main source of higher affinity of DM towards $\alpha_3\beta_4$ nAChR column and observed enantioselectivity in this system, Table 1.

4.3. Functional activity of the DM and LM at the $\alpha_3\beta_4$ nAChR

In order to determine whether the enantioselective retention of DM and LM on the CMAC ($\alpha_3\beta_4$ nAChR) column reflected a functional difference between DM and LM, nicotine stimulated $^{86}Rb^+$ efflux studies were conducted using stably transfected KX$\alpha_3\beta_4$R2 cells, the same cell line used to prepare the CMAC column [15]. The results demonstrated that there was no enantiospecific difference in the strength of the inhibitory effect, i.e. IC_{50} values, Table 1. However, there was a difference between the duration of the inhibitory effect, as the LM-treated cells recovered their activity, measured as percent recovery, faster than those treated with DM. The results indicated that the DM-$\alpha_3\beta_4$ nAChR complex was more stable than the LM-$\alpha_3\beta_4$ nAChR complex and, consequently, DM dissociated from the complex at a slower rate than LM. The data from the functional studies were consistent with the results from the NLC studies and indicated that the chromatographic data reflected the actual pharmacological situation and that the observed enantioselectivity in both systems is due to enthalpy differences between the NCI-receptor (selectant–selector) complexes.

4.4. Molecular modeling of DM and LM interactions with nAChR

A model of the central lumen of the $\alpha_3\beta_4$ nAChR was developed to describe the binding and function of NCIs to this receptor [18].

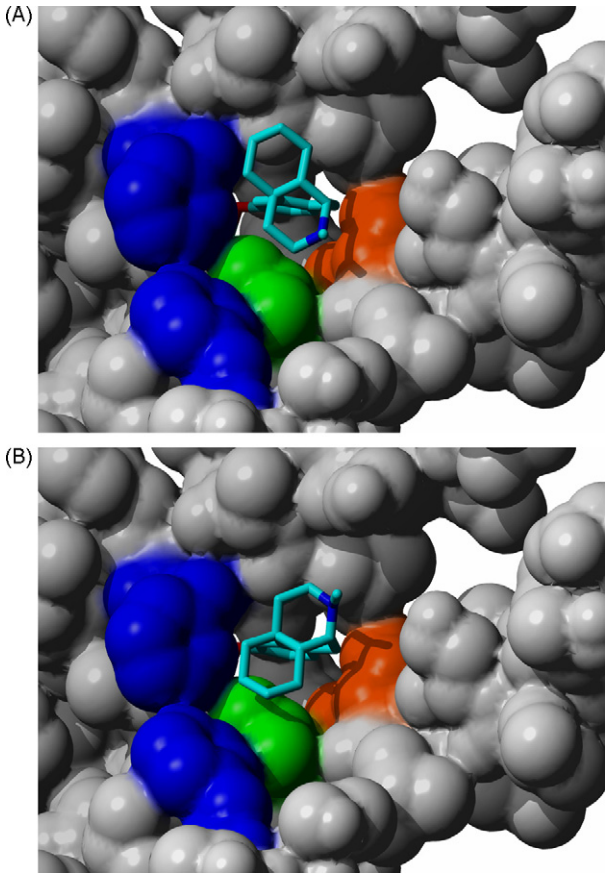

Fig. 2. The most stable docked orientations of (A) dextromethorphan and (B) levomethorphan complexes with the model of the central lumen of the $\alpha_3\beta_4$ nAChR. Hydrophobic clefts formed within the channel are shown in detail. Residues forming the cleft are color coded phenylalanine: blue, valine: green and serine: orange.

The model was built using the homology/comparative approach and began with a model containing five transmembrane M2 segments oriented around the central pore (deposited in RCSB PDB as 2ASG). The final model of the $\alpha_3\beta_4$ nAChR luminal domain contained specific amino acid rings distributed along the channel produced by five amino acids, one from each M2 helix. An extracellular polar ring (E/K) at the edge of the membrane was followed in sequence by three non-polar (L, V/F and L) and then three polar (S, T and intermediate (E)) rings. Position 15 (the V/F ring) is at the narrowest point of the central lumen and the hydrophobic moieties of the amino acid residues the comprise the V/F ring have been defined as the hydrophobic gate of the nAChR. An important feature of the $\alpha_3\beta_4$ nAChR channel is that there are three phenylalanine residues at position 15 (V/F ring), contributed by the β_4 subunits and two isopropyl moieties contributed by the α_3 subunits. The presence of these moieties resulted in the formation of a spatially defined asymmetric hydrophobic cleft between the α_3 and the β_4 helices which is a deep (~6 Å) and oblong (~5 Å) pocket.

In docking simulations using $\alpha_3\beta_4$ nAChR model and DM and LM, the lowest energy docked conformations of the DM and LM complexes were both located at the V/F ring and involved the insertion of the hydrophobic portion of both molecules into the hydrophobic cleft found at this position, Fig. 2A and B. The mirror image relationship between the two enantiomers and their lack of conformational mobility produce two unique orientations. In the case of DM, Fig. 2A, the bridgehead nitrogen atom of the docked molecule is oriented towards S residues located on the α3 helix

at position 8 (S ring). With LM, the bridgehead nitrogen atom was pointing away from the two helices forming the α3 and β4 subunits, Fig. 2B. The orientation of DM increases the probability of H-bond formation between the bridgehead nitrogen and a hydroxyl moiety on S residues, while the orientation of LM reduces this probability as well as the strength of any H-bond interaction that might occur. Using this model, the $\Delta\Delta G_{(n)}$ for the methorphan–nAChR complexes, calculated as $\Delta G_{DM} - \Delta G_{LM}$, was -0.33 kcal mol^{-1} which is in agreement with $\Delta\Delta G^{\circ}$ values determined in the chromatographic experiments.

While the $\alpha_3\beta_4$ nAChR contains three phenylalanines in the luminal binding site (each incorporated by the M2 helix of β4 subtype), the $\alpha_3\beta_2$ nAChR subtype contains five valine residues in these positions [18,40]. A model of the central lumen of the $\alpha_3\beta_2$ nAChR was developed and, as in the $\alpha_3\beta_4$ nAChR, the model contained hydrophobic clefts located at the ring 15 [40]. However, these clefts were shallow depressions (~3 Å deep) with wide round opening (~9 Å wide). When DM and LM were docked in the $\alpha_3\beta_2$ nAChR model the aromatic moieties of both molecules were located in the hydrophobic clefts. Since the clefts were wide and shallow, the molecules were able to move within the clefts in order to optimize the potential for secondary hydrogen bonding interactions, Fig. 3A and B. As a result, the bridgehead nitrogen atoms of both DM and LM have the same probability of forming hydrogen bonds with a hydroxyl moiety on the S ring and the calculated $\Delta\Delta G_{(n)} \approx 0$. The results of the modeling experiments were consistent with the chromatographic results obtained on a CMAC ($\alpha_3\beta_2$ nAChR) column in which there was no difference in the retention times of DM and LM [40].

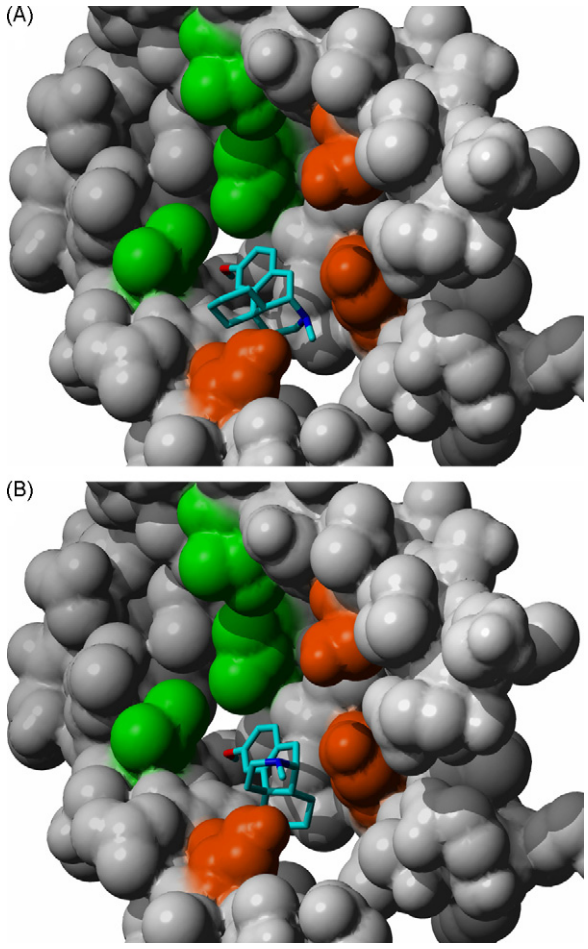

Fig. 3. The most stable docked orientations of (A) dextromethorphan and (B) levomethorphan complexes with the model of the central lumnen of the $\alpha_3\beta_4$ nAChR. Hydrophobic clefts formed within the channel are shown in detail. Residues forming the cleft are color coded valine: green and serine: orange.

4.5. Chiral recognition of DM and LM by the $\alpha_3\beta_4$ nAChR

The results from the studies of the interaction of DM and LM with the CMAC ($\alpha_3\beta_4$ nAChR) column demonstrate that the observed enantioselectivity is the result of the enhanced stability of the DM-$\alpha_3\beta_4$ nAChR complex relative to the LM-$\alpha_3\beta_4$ nAChR complex. This enhancement arises from a hydrogen bond interaction between the bridgehead nitrogen atom on the DM group and a hydroxyl moiety on an S residue located on the α3 helix. The other interaction between DM and LM and the $\alpha_3\beta_4$ nAChR is the insertion of the hydrophobic portion of the methorphan molecule into a defined hydrophobic cleft located within the central lumen of the receptor. Since the methorphan molecules are rigid, the interaction with the hydrophobic cleft is the key interaction as it fixes the positions the bridgehead nitrogen atoms of LM and DM. This assumption was confirmed by the data from the studies utilizing the $\alpha_3\beta_2$ nAChR in which the shallow and less defined hydrophobic area allows enough positional mobility that both the LM and DM are capable of producing the hydrogen bonding interaction, and there is no observed enantioselectivity.

It is tempting to describe the observed enantioselectivty as the result of a two-point interaction mechanism. However, the data could be fit to the TPI mechanism defined by Davankov in which the structure of the inner lumen of the nAChR is designated as a steric restricted environment, thereby adding a third non-bonding (repulsive) interaction [29]. The enantioselectivity can also be explained using the SR model from the point of view of the topology of the surface of the inner lumen [33,34]. These mechanisms are not mutually exclusive, but do not really address the pharmacological process associated with the enantioselective inhibition of nAChR activity.

The agonist-induced opening of the hydrophobic "gate" located at ring 15 of the central lumen has been described as an organized and sequential movement of segments of the protein [41]. When NCIs bind at the hydrophobic clefts, the resulting NCI–nAChR complexes increase the energy of activation required to produce the conformational changes required in the gating process essentially freezing the nAChR in a closed conformation [42]. Since the IC_{50} values associated with the non-competitive inhibition of the $\alpha_3\beta_4$ nAChR by DM and LM are equivalent, Table 1 [15], the data suggests that the insertion of the hydrophobic moiety of the methorphan molecule into the hydrophobic pocket on the nAChR is the key pharmacological interaction, and that this interaction occurs at the same rate and with the same probability for both DM and LM. While the initial binding interaction of DM and LM with the hydrophobic pocket is not enantioselective, it tethers the molecules to the receptor and positions them for the second interaction, the configurationally defining hydrogen bonding interactions. The two steps in the binding process are interconnected and produce a dynamic chiral recognition mechanism.

5. Human organic cation transporter 1 (hOCT1)

5.1. CMAC (hOCT1) columns

The hOCT1 is a member of the Solute Carrier (SLC) 22 superfamily, which has 12 members in humans including the organic cation transporters OCT1, OCT2 and OCT3, the carnitine transporter, and several organic anion transporters. OCTs are believed to mediate the bidirectional transport of small organic cations (50–350 amu) such

Table 2
The K_i value (K_i (Exp)) for competitive inhibitors of TEA transport by the hOCT1 determined using frontal displacement chromatography on a CMAC (hOCT1) column using [^{3}H]-MPP$^+$ as the marker ligand

Compound	*Ki* (Exp) (μM)	α	
		Enantiomers	Diastereomers
(*R*)-Verapamil	0.05		
(*S*)-Verapamil	3.46	69.2	
(*S*)-Atenolol	0.46		
(*R*)-Atenolol	0.98	2.1	
(*S*)-Propranolol	2.85		
(*R*)-Propranolol	0.95	3.0	
(1*R*,2*R*)-Pseudoephedrine	1.12		
(1*S*,2*S*)-Pseudoephedrine	1.71	1.5	
Quinidine	6.33		
Quinine	10.18		1.61
(*S*,*S*)-Fenoterol	3.73		
(*R*,*R*)-Fenoterol	12.6	3.4	
(*S*,*R*)-Fenoterol	6.18		
(*R*,*S*)-Fenoterol	13.2	2.1	
(*R*,*S*)-Fenoterol/(*R*,*R*)-fenoterol			1.1
(*R*,*R*)-Fenoterol/(*S*,*R*)-fenoterol			2.0
(*R*,*S*)-Fenoterol/(*S*,*S*)-fenoterol			3.5
(*S*,*R*)-Fenoterol/(*S*,*S*)-fenoterol			1.7
(*S*)-Isoproterenol	180		
(*R*)-Isoproterenol	120	1.5	
(*R*)-Disopyramide	15.0		
(*S*)-Disopyramide	30.0	2.0	

The enantioselectivities (α enantiomers) and diastereoselectivities (α diastereomers) were calculated as highest K_i/lowest K_i. For experimental details, see [45,48].

as tetraethylammonium (TEA) and 1-methyl-4-phenylpyridinium (MPP$^+$) [43].

A CMAC (hOCT1) column was prepared and characterized using membrane fragments obtained from a stably transfected MDCK cell line, which expresses hOCT1, and the interactions between small molecules and the hOCT1 were studied using frontal affinity chromatography [44]. In these studies the effect of increasing displacer concentration on the chromatographic retention of the marker ligand, [^{3}H]-MPP$^+$ were correlated with the affinity, K_i, of the displacer ligand for the site at which the marker ligand binds. In the initial studies, the K_i values of seven known hOCT1 ligands were obtained using the CMAC (hOCT1) column and were shown to correlate with previously reported K_i values obtained using cellular uptake techniques ($r^2 = 0.9363$; $p = 0.0016$).

5.2. CMAC determined enantioselective binding to the hOCT1

During the initial characterization of the CMAC (hOCT1) column it was observed that (*R*)-verapamil had a 69-fold lower K_i than (*S*)-verapamil. The observed enantioselectivity was consistent with a previous study in which it was demonstrated that the IC_{50} value associated with (*R*)-disopyramide inhibition of hOCT1-mediated uptake of TEA was 2-fold lower than the corresponding IC_{50} of (*S*)-disopyramide [45]. Subsequently the study was expanded to determine the enantioselectivity of the hOCT1 transporter for the enantiomers of verapamil, atenolol, propranolol and pseudoephedrine [19]. The observed enantioselectivities for the three additional enantiomeric pairs ranged from 1.5 to 3.0, Table 2. The data indicate that the interactions with the CMAC (hOCT1) were enantioselective, but to a lesser degree than the selectivity observed with verapamil.

5.3. Functional activity of (R)- and (S)-propranolol at the hOCT1

The chromatographic results were compared with functional inhibition studies utilizing the same stably transfected hOCT1-MDCK cell line used to create the CMAC (hOCT1) column [19]. These experiments examined the effect of (*S*)-propranolol and (*R*)-propranolol on the hOCT1 mediated uptake of TEA. The calculated IC_{50} value associated with (*S*)-propranolol inhibition was 2.75-fold lower than that of (*R*)-propranolol, which was consistent with the chromatographically determined enantioselectivity of 3.0, Table 2. The results indicate that the chromatographically determined K_i values reflect functional interactions with the hOCT1.

5.4. The modeling of stereoselective binding to the hOCT1

A set of 22 compounds including eight pairs of enantiomers and three pairs of diastereomers in Table 2, were used to develop a pharmacophore model to describe the observed stereoselective binding to the hOCT1 [20]. The pharmacophore modeling was carried out using Catalyst version 4.11 and HypoGen and was based upon the correlation of the structures and activities (K_i values) of the compounds used in the study. The resulting model contained a positive ion interaction site, a hydrophobic interaction site and two hydrogen-bond acceptor sites. Using the center of the positive ion interaction site as the origin, the distances to the center the hydrogen-bond acceptor sites are ~3.7 Å (HBA1) and ~8.6 Å (HBA2) and the distance to the center of the hydrophobic site is ~7 Å. The model was able to predict experimentally determined K_i values ($r^2 = 0.6489$, $p < 0.0001$) and the experimentally determined stereoselectivites of the 13 sets of enantiomers/diastereomers ($r^2 = 0.9992$, $p < 0.0001$).

The hOCT1 pharmacophore model was used to explore the basis of the observed stereoselectivities of the model compounds [20]. When (*R*)-verapamil was fit to the proposed pharmacophore, all the relevant functional groups of the molecule matched the hypothesis, Fig. 4a, while (*S*)-verapamil could be mapped to only three of the model feature sites, Fig. 4b. The difference, and therefore the source of the enantioselectivity, was the mapping of the nitrile moiety present on the chiral carbon. The *R*-configuration permitted this interaction with HBA1, while the *S*-configuration did not.

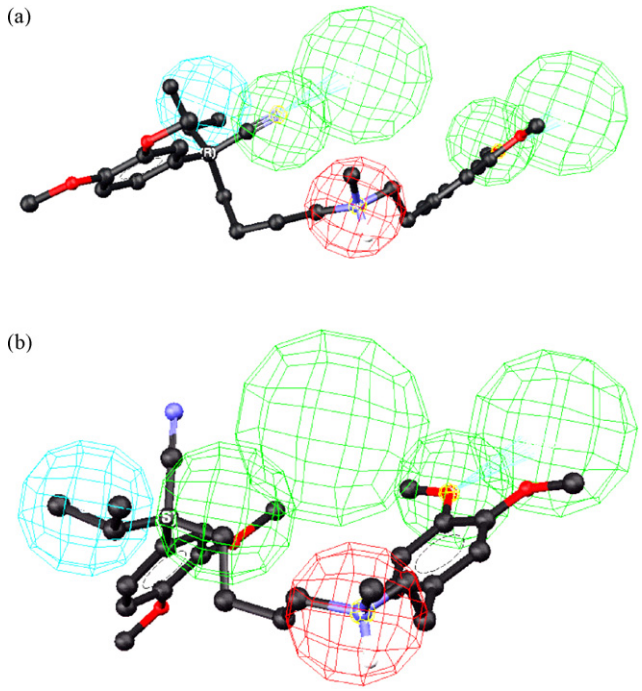

Fig. 4. The fit of verapamil enantiomers in the human organic cation transporter pharmacophore model developed using stereoselective binding data, where (a) the mapping of (*R*)-verapamil; (b) the mapping of (*S*)-verapamil. Reprinted from [48].

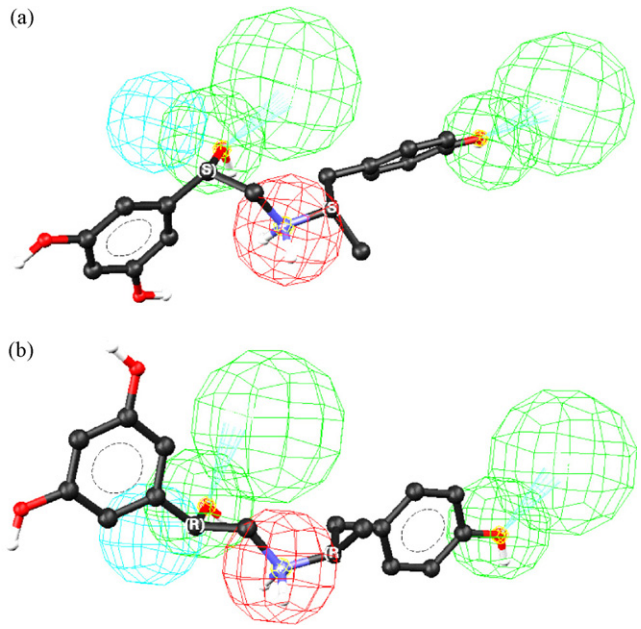

Fig. 5. The mapping of *R*,*R*- and *S*,*S*-fenoterol to a human organic cation transporter pharmacophore in which the red sphere represent a positive ion interaction site, the blue sphere represents a hydrophobic interaction site and the green spheres represent two hydrogen-bond acceptor sites, HBA1 and HBA2; where (a) the mapping of *S*,*S*-fenoterol, (b) the mapping of *R*,*R*-fenoterol. Reprinted from [48].

Thus, the chiral recognition appears to be based upon the ability of (*R*)-verapamil to make an additional stabilizing interaction.

This was not the case when (*R*)- and (*S*)-propranolol were mapped to the pharmacophore. Both enantiomers interacted with the same sites, the positive ion interaction, hydrophobic and HBA1 sites. The difference in the stabilities of the (*R*)-propranolol–hOCT1 and (*S*)-propranolol–hOCT1 complexes, and therefore the source of the enantioselectivity, was the relative fits of the two enantiomers to the model, which were 6.45 for (*R*)-propranolol and 6.31 for (*S*)-propranolol. In the same manner, the mapping of (*S*,*S*)-fenoterol and (*R*,*R*)-fenoterol with the pharmacophore model indicated that for these compounds, a different set of three functional features, the positive interaction site, HBA1 and HBA2, were essential for binding, Fig. 5a and b. As with propranolol, both enantiomers mapped to these sites and the difference in the estimated K_i values was a function of the calculated fits, which were 6.08 for (*S*,*S*)-fenoterol and 5.73 for (*R*,*R*)-fenoterol.

5.5. Chiral recognition by the hOCT1

The ability of the proposed pharmacophore to identify differences in the relative fit between enantiomeric and diastereomeric pairs suggests that the 3-dimensional relationship between the identified interaction sites reflects the spatial distribution of similar binding sites within hOCT1. It also suggests that multiple interactions take place between the selectant and selector which involve multiple locations on both molecules, similar to the topological approach described in the SR model [30,31]. The structure of the hOCT1 pore can also be considered as a steric restricted environment that adds a fourth, or fifth, repulsive interaction, which plays a role in the chiral discrimination mechanism [24].

However, the fact that differences in relative fit produced the experimentally observed stereoselectivities suggests that there is another key component of the chiral recognition mechanism, conformational adjustments by the selectant and selector. The data suggest that for the model compounds, chiral recognition is a multi-step process involving an initial tethering of the selectant to the selector, most probably occurring at the positive ion interaction site, followed by conformational adjustments which produce the optimum interactions. This process results in a distribution of selectant–selector complexes of varying relative stabilities and the observed enantioselectivity. The proposed mechanism is supported by the 2.75-fold lower IC_{50} value of (*S*)-propranolol relative to that of (*R*)-propranolol, which indicates that the inhibition of TEA transport was produced by the final complex not the initial tethering.

It is likely that the observed enantioselective binding of (*R*)- and (*S*)-verapamil occurs in much the same manner. This has been suggested by recent data using point mutated hOCT1 in which the removal of one of the HBA binding sites reduced the observed enantioselectivity to ~4. In the resulting model, both (*R*)-verapamil and (*S*)-verapamil made the same bonding interactions with the new pharmacophore model (unpublished data). Thus, the presence of the second HBA binding site only affected the magnitude of the enantioselectivity, not the source.

6. Conclusions—a dynamic model of chiral recognition

The results from the studies of the enantioselective interactions with the $\alpha_3\beta_4$ nAChR and hOCT1 suggest that the prevailing static point-based chiral recognition models should be amended to reflect the fact that chiral recognition is a dynamic process. The chiral recognition process suggested in the CMAC studies is consistent with a previously proposed conformationally driven chiral recognition mechanism [46–48]. This mechanism was derived from studies of the chromatographic enantioseletive separations of α-alkylcarboxylic acids and mexiletine-related compounds on the amylose tris(3,5-dimethylphenylcarbamate) CSP, which included thermodynamic and molecular modeling approaches [47,48]. In this mechanism, each enantiomer of the selectant interacts with the same sites on the chiral selector and the observed enantioselectivity is a product of a multi-step, interconnected process that results in the differential stabilities of the resulting diastereomeric complexes. The steps involved in this mechanism are described as follows [46].

6.1. Formation of the selector–selectant complex (tethering)

In this step, selectant distributes from the mobile phase to the selector through an initial attractive interaction such as electrostatic, hydrogen bonding, dipole–dipole, etc. Since the physicochemical properties of enantiomers are essentially identical, this interaction tethers the selectant to the selector, but does not, in itself, produce energetically different diastereomeric complexes.

6.2. Positioning of the selector–selectant to optimize interactions (conformational adjustments)

Once the initial complex has been formed, the selecant and selector adjust to each other in order to allow for secondary interactions between the two molecules. These adjustments include simple rotational changes in the conformation of the selectant and/or selector or more significant molecular adjustments. The relative energy required to accomplish the necessary adjustments can play a key role in the enantioselectivity (as with the hOCT1) or none at all (as with the nAChR).

6.3. Formation of secondary interactions (activation of the diasteromeric complex)

As the selectant and selector conformationally adjust to each other, secondary interactions occur which determine the position

of the two molecules relative to each other. This step is also a process that occurs in stages and contributes to the total conformational energy required to produce the final complexes as well as the stabilization/destabilization of the complexes via attractive and repulsive interactions.

6.4. Expression of the molecular fit (stabilizing and destabilizing interactions)

As the secondary interactions occur, the selectant–selector complex can be stabilized by one or more attractive interactions that can include electrostatic, hydrogen bonding, π–π and hydrophobic interactions. At the same time, the selector and selectant are brought closer to each other and repulsive van der Waal interactions may develop or increase in magnitude. The relative stabilities of the two diastereomeric complexes, and, therefore the observed enantioselectivity, will reflect the sum of the stabilizing and destabilizing interactions.

Acknowledgements

This work was supported by funding from the National Institute on Aging Intramural Research Program (IWW) and from the Foundation for Polish Science (FOCUS 4/2006 programme) (K.J.).

References

[1] D. Drayer, in: I.W. Wainer (Ed.), Drug Stereochemistry, Analytical Methods and Pharmacology, 2nd edition, Marcel Dekker, New York, 1993, pp. 5–24.
[2] L. Pasteur, in: G.M. Richardson (Ed.), The Foundation of Stereochemistry, Memoirs of Pasteur, Van 't Hoff, Le Bel and Wislicenus, American Book Co., New York, 1901, pp. 1–33.
[3] W.J. Lough, I.W. Wainer (Eds.), Chirality in Natural and Applied Science, Blackwell Science, Oxford, 2002.
[4] D.J. Triggle, in: W.J. Lough, I.W. Wainer (Eds.), Chirality in Natural and Applied Science, Blackwell Science, Oxford, 2002, pp. 109–138.
[5] W. Lindner, J. LePage, G. Davies, D. Seitz, B.L. Karger, Anal. Chem. 51 (1979) 433.
[6] W. Lindner, J. LePage, G. Davies, D. Seitz, B.L. Karger, J. Chromatogr. 185 (1979) 323.
[7] W. Lindner, C. Petterson, in: I.W. Wainer (Ed.), Liquid Chromatography in Pharmaceutical Development: An Introduction, Aster Publishing, Springfield, OR, 1985, pp. 63–131.
[8] J. Hermansson, J. Chromatogr. 325 (1984) 67.
[9] S. Allenmark, B. Bongren, J. Chromatogr. 252 (1982) 297.
[10] E. Dominici, C. Bertucci, P. Salvadori, G. Felix, C. Cahagne, S. Motellier, I.W. Wainer, Chromatographia 29 (1990) 170.
[11] P. Jadaud, S. Tehlohan, G.R. Schonbaum, I.W. Wainer, Chirality 1 (1989) 38.
[12] I. Marle, P. Erlandsson, L. Hansson, R. Isaksson, C. Pettersson, G. Pettersson, J. Chromatogr. 589 (1991) 233.
[13] S. Patel, I.W. Wainer, J.L. Lough, in: D.S. Hage (Ed.), Handbook of Affinity Chromatography, 2nd edition, Taylor and Francis, Boca Raton, FL, 2006, pp. 571–594.
[14] S. Patel, I.W. Wainer, J.L. Lough, in: D.S. Hage (Ed.), Handbook of Affinity Chromatography, 2nd edition, Taylor and Francis, Boca Raton, FL, 2006, pp. 663–684.
[15] K. Jozwiak, S.C. Hernandez, K.J. Kellar, I.W. Wainer, J. Chromatogr. B 797 (2003) 373.
[16] R. Moaddel, I.W. Wainer, Anal. Chem. Acta 564 (2006) 97.
[17] R. Moaddel, K. Jozwiak, I.W. Wainer, Med. Res. Rev. 27 (2007) 713.
[18] K. Jozwiak, S. Ravichandran, J.R. Collins, I.W. Wainer, J. Med. Chem. 47 (2004) 4008.
[19] R. Moaddel, S. Patel, K. Jozwiak, R. Yamaguchi, P.C. Ho, I.W. Wainer, Chirality 17 (2005) 501.
[20] R. Moaddel, S. Ravichandran, F. Bighi, R. Yamaguchi, I.W. Wainer, Br. J. Pharmacol. 151 (2007) 1305.
[21] E.H. Easson, E. Stedman, Biochem. J. 27 (1933) 1257.
[22] C.E. Dalgliesh, J. Chem. Soc. (1952) 3940.
[23] W.H. Pirkel, M.H. Hyun, B.A. Bank, J. Chromatogr. 316 (1984) 585.
[24] V.A. Davankov, Chirality 9 (1997) 99.
[25] V.I. Sokolov, N.S. Zrfriov, Dokl. Akad. Nauk. SSSR 319 (1991) 1382.
[26] S. Garten, P.U. Biedermann, I. Agranat, S. Topiol, Chirlaity 17 (2005) S159.
[27] R. Kafri, D. Lancet, Chirality 16 (2004) 369.
[28] A.D. Mesecar, D.E. Koshland Jr., Nature 403 (2000) 614.
[29] A. Del Rio, J.M. Hayes, M. Stein, P. Piras, C. Roussel, Chirality 16 (2004) S1.
[30] V. Sundaresan, R. Abrol, Protein Sci. 11 (2002) 1330.
[31] V. Sundaresan, R. Abrol, Chirality 17 (2005) S30.
[32] J.-P. Changeux, D. Bertrand, P.J. Corringer, S. Dahaene, S. Edelstein, C. Lena, N. Le Novere, L. Marubio, M. Piccioto, M. Zoli, Brain Res. Rev. 26 (1998) 198.
[33] A. Karlin, Nat. Res. Neurosci. 3 (2002) 102.
[34] J.-P. Changeux, J.L. Galzi, A. Devillers-Thiery, D. Bertrand, Q. Rev. Biophys. 25 (1992) 395.
[35] R. Moaddel, K. Jozwiak, R. Yamaguchi, C. Cobello, K. Whittington, T. Sakur, S. Basak, I.W. Wainer, J. Chromatogr. B 813 (2004) 235.
[36] K. Jozwiak, R. Moaddel, R. Tamaguchi, A. Maciuk, I.W. Wainer, Pharm. Res. 23 (2006) 2175.
[37] J.L. Wade, A.F. Bergold, P.W. Carr, Anal. Chem. 59 (1987) 1286.
[38] T. Fornstedt, G. Guiochon, Anal. Chem. 73 (2001) 608A.
[39] Peak Fit for Windows, version 4.11, SPSS Inc, Chicago, IL, 2001.
[40] K. Jozwiak, S. Ravichandran, J.R. Collins, R. Moaddel, I.W. Wainer, J. Med. Chem. 50 (2007) 6279.
[41] N.S. Millar, Biochem. Soc. Trans. (2003) 869.
[42] R. Moaddel, K. Jozwiak, K. Whittington, I.W. Wainer, Anal. Chem. 77 (2005) 895.
[43] H. Koepsell, B.M. Schmitt, V. Gorboulev, Rev. Physiol. Biochem. Pharmacol. 150 (2003) 36.
[44] R. Moaddel, R. Yamaguchi, P.C. Ho, S. Patel, C.P. Hsu, V. Subrahmanyan, I.W. Wainer, J. Chromatogr. B 818 (2005) 263.
[45] L. Zhang, M.E. Schaner, K.M. Giacomini, J. Pharmacol. Exp. Ther. 286 (1998) 354.
[46] T.D. Booth, D. Wahnon, I.W. Wainer, Chirality 9 (1997) 96.
[47] T.D. Booth, I.W. Wainer, J. Chromatogr. A 737 (1996) 157.
[48] T.D. Booth, I.W. Wainer, J. Chromatogr. A 741 (1996) 205.